Computational Study on the Charge Mixing of Internal Exhaust Gas Recirculation Initiated Controlled Auto Ignition

Paul Osei-Owusu, Rui Chen, and Salah Ibrahim
Department of Aeronautical and Automotive Engineering, Loughborough University, UK

SYNOPSIS

Controlled Auto Ignition (CAI) uses compression heat to auto ignite a homogeneous air/fuel mixture. Using internal exhaust gas re-circulation (IEGR) as an indirect control method, CAI offers potentially superior fuel economy and pollutant emission reductions. The local chemical and thermal conditions of the engine charge towards the end of the compression stroke have significant influences toward fuel auto ignition performance. In this study, KIVA-3V has been employed to investigate the mixing process involving the fuel, air and the IEGR inside a pentroof engine. The calculated results were compared with experimental data. A mixing index was formulated to show the level of homogeneity in the mixture during the compression process. Good correlations were obtained between the measured and calculated data. Results showed that the level of mixing between trapped burnt gas and the fresh mixture is enhanced by increasing the percentage of trapped IEGR.

1. INTRODUCTION

Controlled Auto Ignition (CAI) compared to gasoline engines has the potential to be highly efficient, leading to lower emissions than conventional spark ignition (SI). The CAI engines can have efficiencies as high as compression ignition (CI) engines, while producing ultra-low oxides of nitrogen (NO_X) and particulate matter (PM) emissions [1,2,3]. In basic terms they represent the next major step beyond CI and SI engines for use in transportation vehicles. CAI engines incorporate the best features of both SI and CI engines as well as able to operate on gasoline, diesel fuel, and most alternative fuels [1].

The mixture in a CAI event can be achieved by mixing the fuel and air in the intake port, or by injecting fuel directly into the cylinder at a very early stage in the cycle. It is now generally agreed that CAI combustion is dominated by local chemical-kinetic reaction rates [2,5] with no requirement for flame propagation. If a truly homogeneous mixture exists at the time of combustion, it is considered that the turbulence has little direct effect on CAI combustion, but it may have an indirect effect on altering the temperature distribution and the boundary layer thickness within the cylinder. Small temperature differences inside the cylinder have a considerable effect on combustion due to the sensitivity of chemical kinetics to temperature. As a result, heat transfer and mixing are important in forming the optimum condition of the charge prior to ignition, although they play a secondary role during the CAI combustion process itself due to its ultra-high heat release rate.

Modelling of CAI until recently has generally lagged behind experimental work. However, with the understanding of the fundamentals and advances in computational power, more researchers have begun to provide in-depth descriptions of CAI combustion. These models, depending on their intended use, have been developed using different descriptions for both the in-cylinder and the engine process. A survey of the CAI/Homogeneous Charge Compression Ignition (HCCI) literature has shown that model development in the field tends to focus on the following approaches:

1. Zero-dimensional thermo-kinetic
2. Multi-dimensional approach
3. Segregated, sequential fluid mechanic - thermo-kinetic multi-zone

The basic modelling approach is the zero-dimensional thermo-kinetic approach. This assumes that the fluid mechanics have no implications on the combustion event, aside from possible heat transfer effects. Examples of this approach are the models reported by Christensen [4,6]. In an attempt to improve the single-zone modelling approach, Fiveland and Assanis [7] have reported the development of a complete, four-stroke cycle simulation that integrates complex chemical kinetic mechanisms with physical models of gas exchange and in-cylinder processes, including turbulence and heat transfer. Overall, while zero-dimensional models have shown the ability to provide satisfactory accuracy against measurements of engine performance, they are considered to suffer when predicting the rate of heat release, combustion completeness, and emissions.

Attempts have been made to use three-dimensional computational fluid dynamics (CFD) models coupled with detailed chemistry to study compression ignition under CAI like-conditions. Agarwal and Assanis [8], reported on the coupling of a detailed chemical kinetic mechanism for natural gas ignition, which included 22 species and 104 elementary reactions, with the multi-dimensional reacting flow code KIVA-3 to explore the auto-ignition of natural gas injected in a quiescent chamber under diesel-like conditions. Kong et al [9] also proposed a more practical approach to account for the turbulent effects on prediction of ignition by proposing a reaction rate incorporating the effects of both chemical kinetics and turbulent mixing through characteristic timescales.

In order to retain some of the resolution given by CFD models and reduce the computational time, a segregated, sequential multi-zone modelling approach was proposed by Aceves et al [5,10]. In the latter, a computational fluid dynamics code is run over part of the engine cycle, typically from bottom dead centre (BDC) until a transition point before top dead centre (TDC), and then the fluid is divided into mass-temperature groups. Each temperature group is solved within the context of a single zone, but the groups are solved simultaneously. The model shows promise in capturing inhomogeneities in the temperature field, resulting from heat losses occurring near the wall and in the crevices.

The objectives of this work are to utilise KIVA-3V, to investigate the mixing process among the fuel, air and the IEGR during the intake and compression processes, and characterise a methodology for assessing the homogeneity of the fresh charge with the IEGR inside the cylinder.

2. SIMULATION STUDY

The technique used to initiate and control the CAI in the experimental study was to trap a pre-defined quantity of exhaust gas using a very early exhaust valve closure (EVC) event coupled to a very late inlet valve opening (IVO) event on a single-cylinder research engine equipped with Lotus' Research Active Valve Train (AVT) System. The valve lift was reduced to 6mm to reduce the valve dynamic loading to an acceptable level. Using symmetrically advanced EVC and retarded IVO timings, various amount of IEGR was trapped inside the combustion chamber. The general principle can be seen in Figure 1 [11]. The trapped exhaust gas was then compressed during the final stages of the exhaust stroke. As the piston descends on the induction stroke, the inlet valves were opened and the fresh

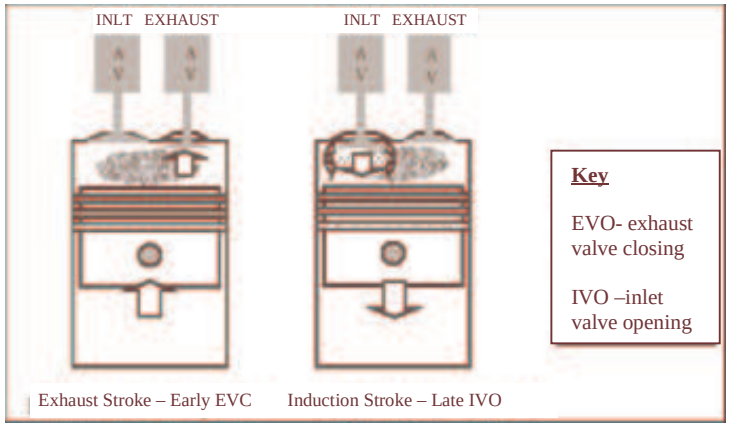

Fig.1 Valve events suitable for CAI combustion

charge was drawn into the cylinder partially filled with exhaust gas. At the end of the induction stroke, the inlet valves were closed and the fresh-charge and exhaust gas mixture compressed. CAI combustion occurs as the mixture ramps up in temperature in the final stages of the compression stroke. Once CAI has occurred, the power stroke drives the piston down and the cycle is repeated.

The centre interest of this research work is to investigate the local air, fuel and IEGR mixture conditions prior fuel auto ignition. Only induction and compression strokes during a CAI combustion process were therefore simulated. In order to supply the model with reasonable initiation conditions to calculate the mixing mechanism insider the cylinder, some engine experimental results were introduced into the model.

The calculations were performed using a 4-Valve Pentroof (an angle of 140°) engine geometry. The rest of engine geometry parameter was: Bore = 92mm, stroke = 85 with a compression ratio of 10:1. These geometric parameters are slightly different from the actual engine used in the experiments. However, since the purpose of using the experimental results was to initiate the start of modelling. The obtained mixing results from the model simulation will still be able to explain the mixing mechanism in the real world. Table 1 listed the initial conditions input into the simulation model obtained from the experimental study.

Study	IEGR (%)	Wall Temperature (K)	In-Cylinder Temperature (K)	Exhaust Temperature (K)	IVO CA (Degrees)	EVC CA (Degrees)
Case 1	36	393.69	881.79	761.25	425	295
Case 2	39	394.21	872.31	751.25	428	292
Case 3	41.5	395.03	862.21	741.05	431	289
Case 4	44.3	395.65	854.05	731.55	434	286
Case 5	47	397.19	848.99	724.95	437	283
Case 6	49.8	399.06	841.86	715.95	440	280
Case 7	52.5	400.19	840.29	713.25	443	277
Case 8	55.2	402.14	839.14	710.15	446	274
Case 9	57.9	402.24	837.64	708.55	449	271

Table 1: Initial modelling conditions

All calculations were performed at a fixed engine speed of 2000rpm. The simulation started at EVC. The pressure and temperature of the trapped gas inside the cylinder at this crank angle position were taken from experimental results. The wall temperatures introduced into the calculation were obtained from experimental results and were assumed to remain constant during the calculated cycle. For the initial conditions, the engine charge in the intake manifold was assumed to be a homogeneous fresh charge, and the in-cylinder was homogeneous exhaust gas (IEGR) with a uniform pressure and temperature.

The maximum number of grid cells at BDC was about 60,000 cells. Figure 2 shows an example of the grid being used. It has been found that that cell density did not lead to noticeable differences in the calculated temperature field [12]. However, central processing unit (CPU) time was greatly reduced by using coarse grids whilst maintaining sufficient accuracy in combustion and emissions predictions. Therefore, this study considers 60 000 cells to be sufficient.

3. RESULTS AND DISCUSSION

In order to explore and analyse the output data from the KIVA-3V calculations for temperature, H_2O and CO_2 distribution inside the cylinder during the induction and compression processes, a methodology needs to be developed to characterise the mixture homogeneity. This is based on defining a mixing index among the fresh air, fuel, and the trapped IEGR, which represents the number of cells having high temperature or H_2O density or CO_2 density than average level.

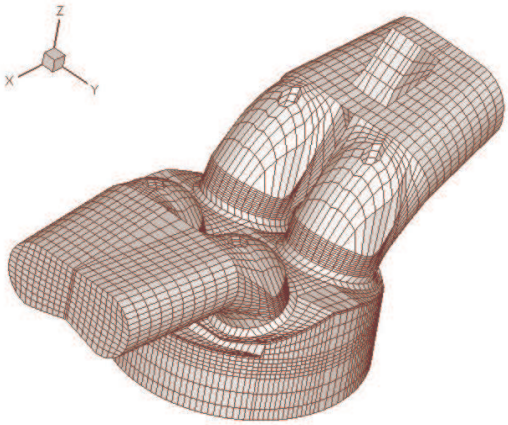

Fig 2: The computational grid used in the current study (shown is the grid at 60° BTDC)

The averages for in-cylinder temperature, H_2O density or CO_2 density were calculated as follows:

$$\bar{a} = \frac{\sum_{i=1}^{n_{cells}} a_i}{n_{Total}} \tag{1}$$

where:
$\bar{a}$ = average temperature inside cylinder, H_2O density or CO_2 density
a_i = cell temperature, H_2O density or CO_2 density
n_{cells} = number of cells
n_{total} = total number of cells within the cylinder

Since the auto ignition can only occur when a certain level of temperature has been reached, it is therefore the interest to investigate the distribution of the temperature above the average. Again, the H_2O and CO_2 are the main components of the IEGR, their distribution above the average values were also studied. The cells with the value above the average, the so called positive cells, were identified by:

$$Postive\ Cells = \sum_{i=1}^{n_{cells}} b_i \left\{ \begin{matrix} b_i=1 \\ b_i=0 \end{matrix} \middle| \begin{matrix} a_i \geq \bar{a} \\ a_i < \bar{a} \end{matrix} \right\} \tag{2}$$

where:
b_i = Number of positive cells above $\bar{a}$

Once the positive cells were identified, they were split into groups to see how the cells deviate from the averages. A two percent increment was used for the temperature and a six percent increment used for H_2O and CO_2 densities to define each group. The mixing index of each group can then be obtained as

$$Mixing\ Index = \frac{n_i}{n_{Total}} \tag{3}$$

where:
n_i is the number of cells counted for the individual groups, and n_{Total} is the total number of cells of the entire cylinder where both inlet and exhaust manifolds are excluded.

The mixing index served as a tool that can be used to characterise the mixture homogeneity. This mixing index has been used below to analyse the data obtained from the simulation. Figure 3 shows the computed and experimental in-cylinder pressure against the crank angle. Both graphs show a peak cylinder pressure of slightly above 14 bar with the shaping mirroring each other. Good correlations

were obtained between the measured and calculated data. For the computed plot, the profile starts at 295CA with 36% of IEGR down to 271CA with 57.9% IEGR. These locations are the EVC timing used to initiate the CAI combustion and are the starting position of the calculation. It demonstrates that in both cases, as the level of IEGR increases, the in-cylinder pressure increases.

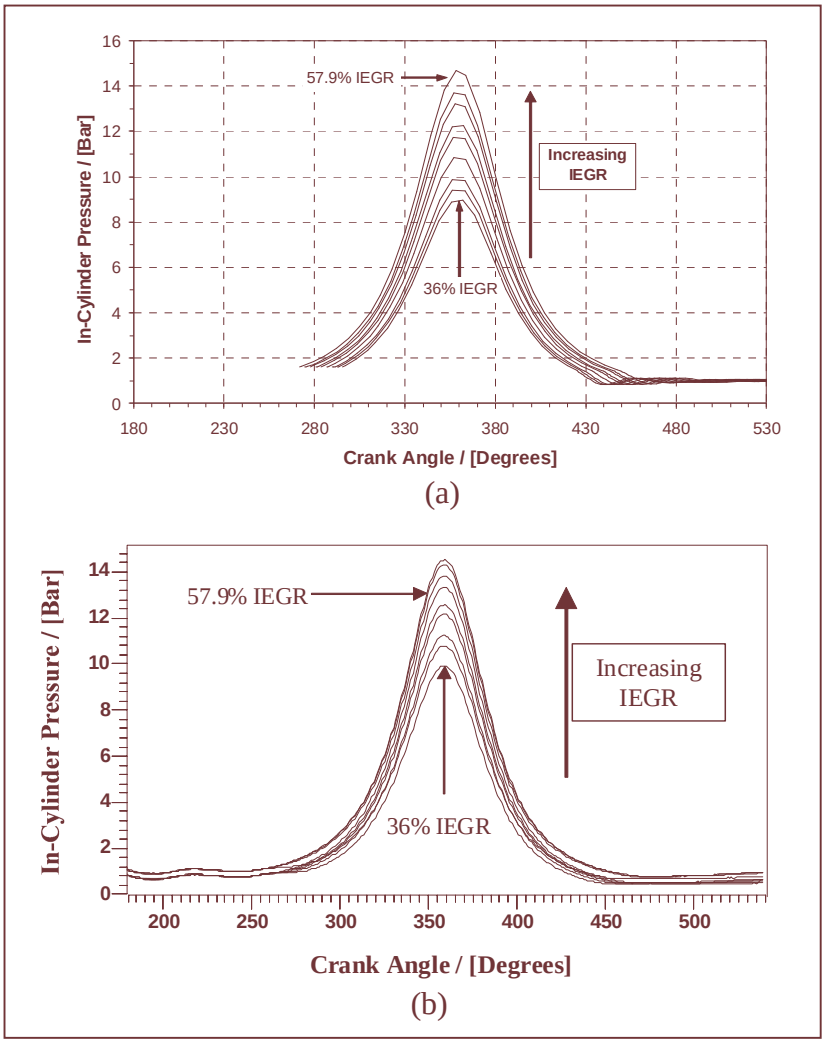

Fig 3: Cylinder pressure vs. crank angle (a) computed (b) experiment

To capture the image of initial modelling conditions which have been highlighted in Table 1, Figure 4 has been plotted.

Figure 4a shows one of the calculated results with 49.8% IEGR. The initial conditions of the calculation were given in the Table 1. It is assumed that a Stoichiometric air/fuel mixture was used in the intake port, the IEGR trapped in the cylinder was consisted of complete combustion products, and the exhaust port has a constant temperature as given in Table 1 throughout the cycle calculation.

At the BDC (540CA) position, the opening of the inlet valve reduces the in-cylinder temperature, and the uniformity of the mixture is lost. Figure 4b shows that a non-uniformed distribution of the in-cylinder temperature occurs. This indicates that the mixture inside the cylinder becomes in-homogeneous as the fresh air and fuel is charged into the cylinder which is initially in a homogeneous condition.

Once the inlet valve closes and the mixture is compressed, the homogeneity of the temperature distribution improves. This can be seen Figure 4c (640CA). As the piston moves further upwards, the homogeneity further improves. However, when the piston reaches the TDC position (720CA), it has been found that the mixture inside the cylinder is still a certain level away from homogeneous, as shown in Figure 4d. The region close to the exhaust valve appears to be hottest, while the region close to the inlet valve appears to be colder than the central part.

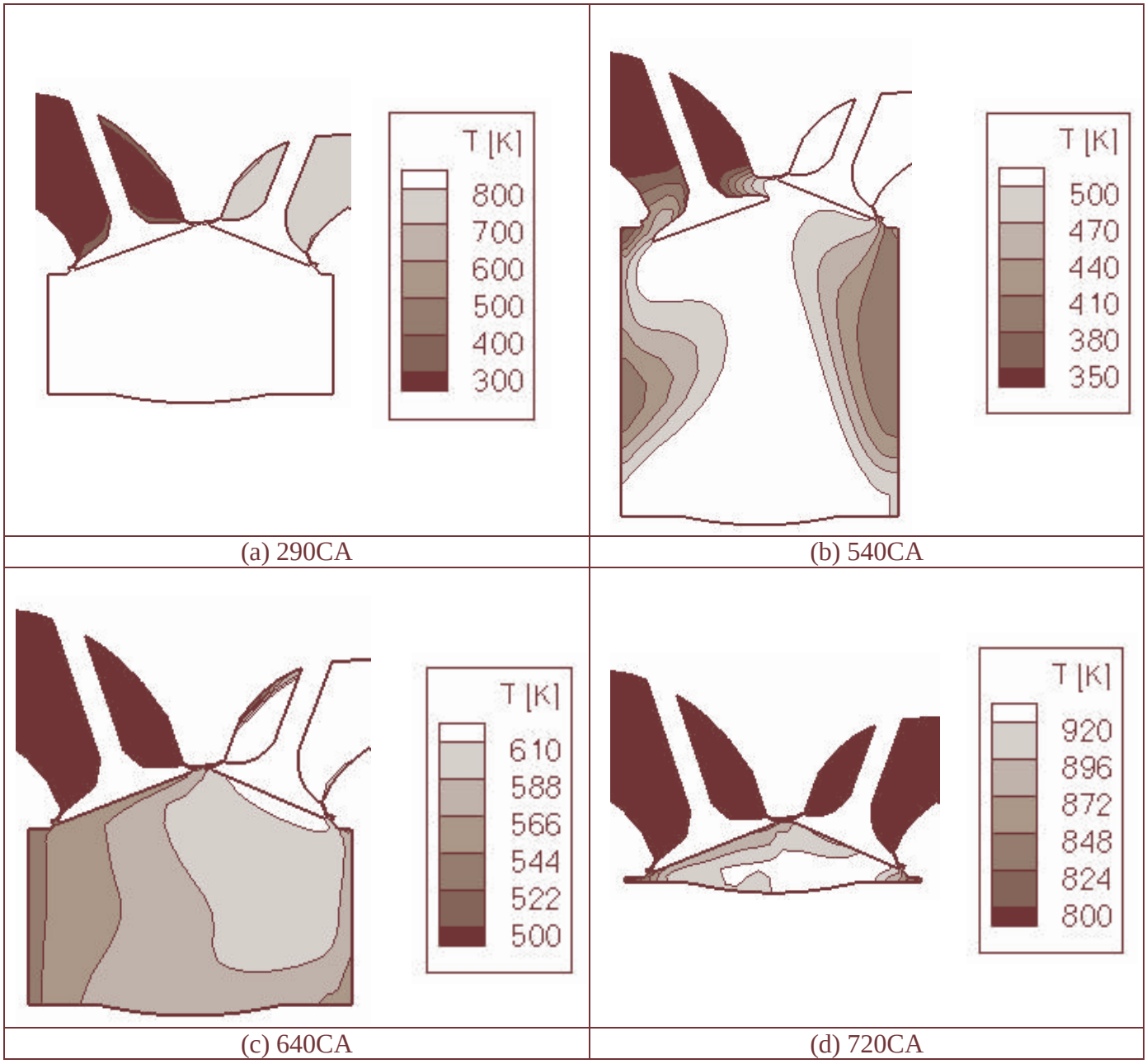

(a) 290CA | (b) 540CA

(c) 640CA | (d) 720CA

Fig 4: Temperature profile at different crank angles (a) shows the initial conditions for start of calculation (b) BDC (c) 630 crank angle (d) end of compression stroke

Figure 5 shows the average in-cylinder temperature and the calculated mixing index. It can be seen that the average temperature increases as IEGR increases. This is because as the IEGR increases the temperature of the bulk gas mixture increases. In a similar trend, as the IEGR increases, the temperature mixing index for the highest grade between 10%-12% above average, increases, too. It indicates that the number of the cells with the highest temperature also increases. This means that as the IEGR is increased, the temperature of the mixture is increased, which in turn increase the total number of cells which has a greater temperature than the average one. The hotter ones will start the auto ignition first, and the increase in their number makes the auto ignition stronger.

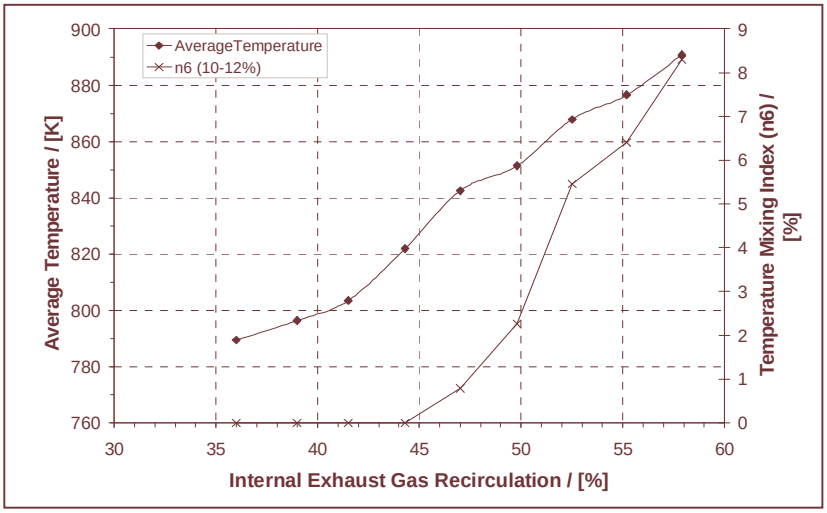

Fig 5: In cylinder average temperature and temperature mixing index vs. IEGR at 720 crank angle

Figure 6 shows all seven calculated grades of the temperature mixing index at varying IEGR. It is interesting to note that the different temperature grades vary differently as the IEGR increases. Grade 1 and 2, which represent the number of cells with a temperature of 0 to 4% above the average value, generally decreases as the IEGR increase. This indicates that as the IEGR increases, less cells have the temperature close to the average level. In other words, the cells' temperature deviate further from the average value as the IEGR increases.

On the other hand, grade 6 and 7 represents the cell number with a temperature of 10 to 14% higher than the average. It can be seen that both grades increase as the IEGR increases. Such a phenomenon represents the fact that as the IEGR increases, the number of the cells with the highest temperature increases, and the auto ignition improves.

Grade 3, 4 and 5 are the grades representing the cell number in the middle of these two extremes. Grade 3 represents the number of cells with a temperature of 4 to 6% higher than the average. As the IEGR increases, it remains more or less unchanged. Grade 4 represents the cell number with a temperature of 6 to 8% higher than average. When the IEGR initially increases, it decreases. However, when the IEGR further increases to a level above 55%, it starts to increase sharply. Grade 5 represents the cell number with a temperature of 8 to 10% higher than average. It mirrors with the grade 4 as the IEGR increases.

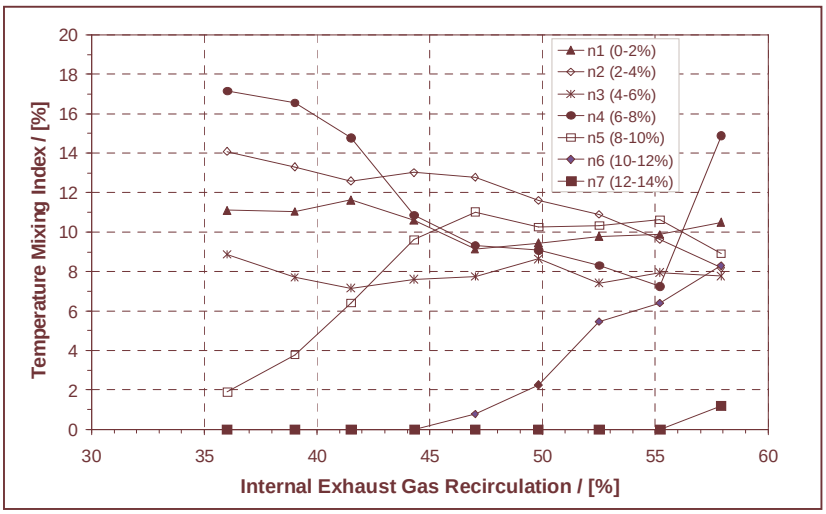

Fig 6: Temperature mixing index vs. IEGR

H_2O and CO_2 are the typical chemical species contained main in the IEGR. Their distribution inside the cylinder is therefore a good indication on the mixing between fresh charge and the IEGR. The mixing index's for both H_2O and CO_2 were calculated and plotted in Figure 7a and 7b, respectively. All 6 calculated grades of the H_2O and CO_2 mixing index at varying IEGR were shown in the Figure. It can be seen that the mixing indexes for H_2O and CO_2 have a very similar variation trend against varying amount of IEGR.

For distribution of both H_2O and CO_2 species which further indicates the distribution of the IEGR inside the cylinder, the calculated mixing grades varying differently as the amount of IEGR changes. As the IEGR increases, grade 1 and 2 increases. Grade 1 and 2 represent 0 to 12% of H_2O and CO_2 density above the average level. In other words, as the IEGR increases, the number of the cells which

have a H_2O or CO_2 density close to average value increases. The system turns to be more homogeneous.

On the other hand, as the IEGR increases, the rest 4 grades either decreases or remain unchanged. These rest grades represent the cells with higher H_2O and CO_2 densities above the average level than grade 1 and 2. Clearly, these results, again, demonstrated that as the IEGR increases, the distribution of H_2O and CO_2 inside cylinder becomes more homogeneous.

4. CONCLUSION

The CFD code KIVA-3V has been used to investigate and identify the charge mixing efficiency at various IEGR levels.

A methodology based on defining a mixing index among the fresh air, fuel, and the trapped IEGR has been defined. It represented the number of cells having high temperature or H_2O density or CO_2 density than average level.

The calculated results showed that as the IEGR increases, fewer cells have the temperature close to the average level. In other words, the cells' temperature deviate further from the average value as the IEGR increases, which agrees with the fact that as the IEGR increases, the number of the cells with the highest temperature increases, and the auto ignition improves.

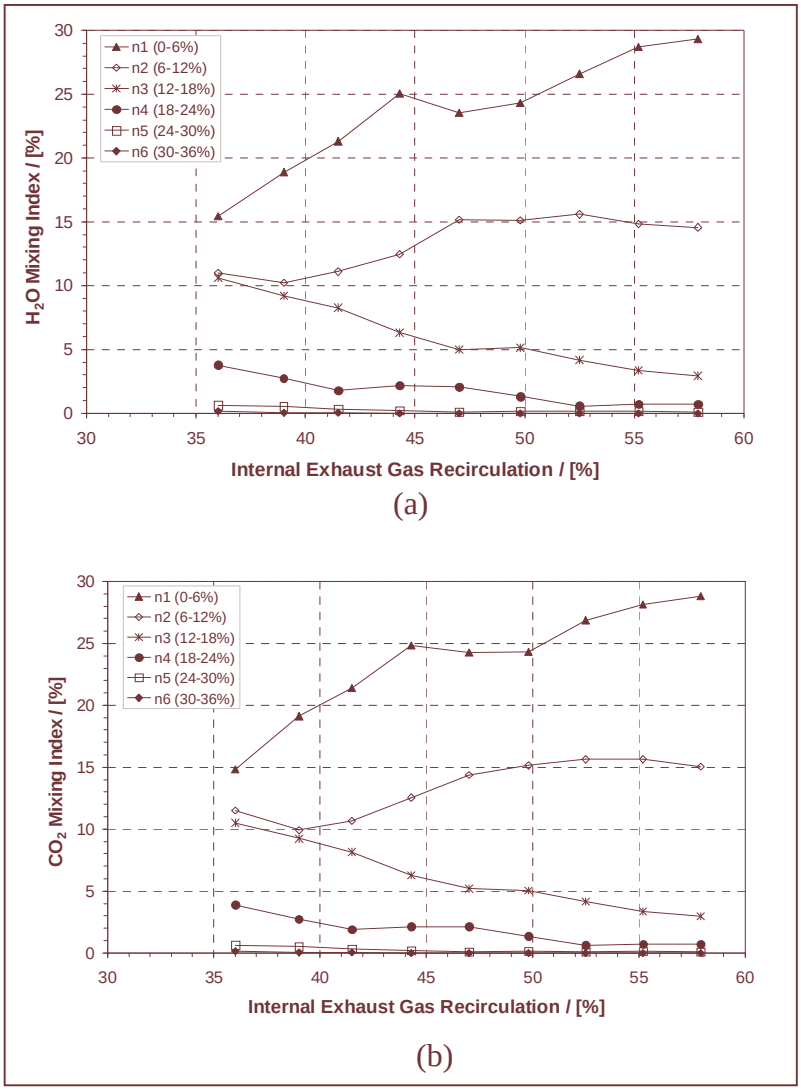

Fig 7: Mixing index plots vs. IEGR (a) H_2O index (b) CO_2 index

H_2O and CO_2 are the typical chemical species contained main in the IEGR. Their distribution inside the cylinder is therefore a good indication on the mixing between fresh charge and the IEGR. The mixing index calculations showed that as the IEGR increases, the number of the cells which have a H_2O or CO_2 density close to average value increases. The system turns to be more homogeneous.

5. ABBREVIATIONS

AVT	Active Valve Train
ATDC	Top Dead Centre
BDC	Bottom Dead Centre
BTDC	Before Top Dead Centre
CA	Crank Angle
CAI	Controlled Auto-Ignition

CFD	Computational Fluid Dynamics
CI	Compression-Ignition
CO_2	Carbon Dioxide
CPU	Central Processing Unit
EVC	Exhaust Valve Closing
EVO	Exhaust Valve Opening
H_2O	Water
HCCI	Homogeneous Charge Compression Ignition
IEGR	Internal Exhaust Gas Recirculation
IVC	Inlet Valve Closing
IVO	Inlet Valve Opening
NO_X	Oxides of Nitrogen
PM	Particulate Matter
SI	Spark-Ignition
TDC	Top Dead Centre

6. REFERENCES

[1] ONISHI, S., JO, S.H., SHODA, K., JO, P.D. and KATO, S., Active Thermo-Atmosphere Combustion (ATAC) - A New Combustion Process for Internal Combustion Engines. (SAE 790501).

[2] NAJT, P.M. and FOSTER, D.E., Compression-Ignited Homogeneous Charge Combustion. (SAE 830264).

[3] BLARIGAN, P.V., PARADISO, N. and GOLDSBOROUGH, S., Homogeneous Charge Compression Ignition with a Free Piston: A New Approach to Ideal Otto Cycle Performance. (SAE 982484).

[4] CHRISTENSEN, M., JOHANSSON, B., AMNEUS, P. and MAUSS, F., Supercharged Homogeneous Charge Compression Ignition. 1998

[5] ACEVES, S., FLOWERS, D., MARTINEZ-FRIAS, J., SMITH, J.R. and DIBBLE, R., Numerical and Experimental Studies of HCCI combustion, August 20-24, 2000

[6] DEC, J.E., A Computational Study of the Effects of Low Fuel Loading and EGR on Heat Release Rates and Combustion Limits in HCCI Engines. (SAE 2002-01-1309).

[7] FIVELAND, S.B. and ASSANIS, D.N., 2000. A Four-Stroke Homogeneous Charge Compression Ignition Engine Simulation for Combustion and Performance Studies. (SAE 2000-01-0332).

[8] AGARWAL, A. and ASSANIS, D.N., Multi-Dimensional Modelling of Natural Gas Ignition Under Compression Ignition Conditions Using Detailed Chemistry. (SAE 980136).

[9] KONG, S.C., MARRIOTT, C.D., REITZ, R.D. and CHRISTENSEN, M., Modelling and Experiments of HCCI Engine Combustion Using Detailed Chemical Kinetics with Multidimensional CFD. (SAE 2001-01-1026).

[10] ACEVES, S.M., FLOWERS, D.L., MARTINEZ-FRIAS, J., SMITH, J.R., WESTBROOK, C.K., PITZ, W.J., DIBBLE, R., WRIGHT, J.F., AKINYEMI, W.C. and HESSEL, R.P., A Sequential Fluid-Mechanic Chemical-Kinetic Model of Propane HCCI Combustion. (SAE 2001-01-1027).

[11] CHEN, R., TURNER, J. and BLUNDELL, D., 2004. The Transition between Controlled Auto Ignition and Spark Ignition. (SAE 2004-01-0939).

[12] KONG, S.C. and REITZ, R.D., A Numerical Study of Premixed HCCI Engine Combustion and its Sensitivity to Computational Mesh and Model Uncertainties. Institute of Physics Publication; Combustion Theory and Modelling. Combust. Theory Modelling 7 (2003) 417–433 PII: S1364-7830(03)53147-3.